



Electromagnetic radiation field of an electron avalanche

Vernon Cooray^{a,*}, Gerald Cooray^b

^a Uppsala University, Uppsala, Sweden

^b Karolinska Institute, Stockholm, Sweden

ARTICLE INFO

Article history:

Received 4 February 2011

Received in revised form 1 June 2011

Accepted 2 June 2011

Keywords:

Electron avalanches

Radiation fields

Microwave radiation

Electrical discharges

Lightning

ABSTRACT

Electron avalanches are the main constituent of electrical discharges in the atmosphere. However, the electromagnetic radiation field generated by a single electron avalanche growing in different field configurations has not yet been evaluated in the literature. In this paper, the electromagnetic radiation fields created by electron avalanches were evaluated for electric fields in pointed, co-axial and spherical geometries. The results show that the radiation field has a duration of approximately 1–2 ns, with a rise time in the range of 0.25 ns. The wave-shape takes the form of an initial peak followed by an overshoot in the opposite direction. The electromagnetic spectrum generated by the avalanches has a peak around 10^9 Hz.

© 2011 Elsevier B.V. All rights reserved.

1. Introduction

A wide variety of electrical discharges takes place in the Earth's atmosphere. According to their spatial dimensions, electrostatic discharges, whose length is measured in millimeters, lie at one end of the spectrum, and lightning discharges, with lengths spanning several tens of kilometers, lie at the other. The measured or calculated electromagnetic fields generated by these electrical discharges are available in literature (Rakov and Uman, 2003; Cooray, 2003a; Gardner, 1990; Chauzy and Kably, 1989.). Despite their evident differences, all atmospheric discharges are initiated and maintained by the same mechanism, that of the electron avalanche (Townsend, 1915; Gallimberti, 1979). Electron avalanches may take place either as an isolated discharge process, for example in corona discharges, or as the precursor of other discharge processes such as streamers and leaders (Loeb, 1955; Les Renardières Group, 1972). Streamers and leaders are the main constituents of electrical sparks at atmospheric pressures (Gallimberti, 1979; Les Renardières Group, 1972). Notwithstanding the important role played by electron avalanches in almost all discharge processes in the

atmosphere and the knowledge available concerning their mechanism (Townsend, 1915; Gallimberti, 1979), it has not been possible to find a single work in the literature that has attempted to calculate the electromagnetic fields generated by electron avalanches. Thus, in this paper we address this issue by evaluating the electromagnetic fields generated by electron avalanches developing in different background electric field configurations.

There are various ways to calculate the electromagnetic fields generated by a discharge if the variation of the current in the discharge is given as a function of space and time (Thottappillil and Rakov, 2001; Cooray, 2003b). In a recent paper, Cooray and Cooray (2010) demonstrated that the electromagnetic fields of accelerating charges could be used to evaluate the electromagnetic fields from electrical discharges if the temporal and spatial variations of the charges in the discharge are known. They compared and contrasted this technique with other techniques used by researchers and showed that even though the total electromagnetic fields calculated do not depend on the technique used, the different techniques provide different insights into the physical problem under consideration. The mere fact that electron avalanches consist of electrons accelerating and decelerating in a given background electric field, makes it convenient to use the approach introduced by the Cooray and Cooray

* Corresponding author.

E-mail address: Vernon.Cooray@angstrom.uu.se (V. Cooray).

(2010) in evaluating the electromagnetic fields of electron avalanches. In this paper, the equations developed by these authors are used to evaluate the radiation fields of electron avalanches.

2. The mechanism underlying an electron avalanche

Consider a free electron originally at $z=0$ that starts to move under the influence of a background electric field directed along the negative z -axis. If the background electric field is larger than the critical value necessary for cumulative ionization, the electron may produce another electron through ionization collisions and these two electrons in turn will give rise to two more electrons. In this way, the number of electrons increases with increasing z . Assume that the number of electrons at a distance z from the origin is n_z . Let α be the number of ionizing collisions per unit length made by an electron traveling in the direction of the electric field, and let η be the number of attachments over the same length. These parameters are known as Townsend's first ionization coefficient and the electron attachment coefficient, respectively (Townsend, 1915; Gallimberti, 1979). Consider an elementary length of width dz located at a distance z from the origin. In traveling across the length dz , n_z number of electrons will give rise to dn additional electrons. The value of dn is given by

$$dn = n_z \bar{\alpha} dz \tag{1}$$

with $\bar{\alpha} = (\alpha - \eta)$. The solution of this equation is

$$n_z = e^{\bar{\alpha}z} \tag{2}$$

This equation shows that the number of electrons increases exponentially with distance and such an exponential growth of electrons with distance is called an electron avalanche (Townsend, 1915; Gallimberti, 1979; Loeb, 1955). The equation also shows that cumulative ionization is possible only if $\bar{\alpha} > 0$. The quantity $\bar{\alpha}$ is known as the effective ionization coefficient and its magnitude depends on the electric field; its value is negative for fields less than about 2.8×10^6 V/m in atmospheric air (Gallimberti, 1979; Raizer, 1991). Since the value of $\bar{\alpha}$ depends on the background electric field, the growth and demise of an electron avalanche depends on the spatial variation of the background electric field. When the avalanche propagates in the background electric field, cumulative ionization takes place at the head of the avalanche, unless the background electric field decreases below about 2.8×10^6 V/m, in which case, the ionization ceases. If the background electric field continues to decrease, then the number of electrons in the avalanche may continue to decrease as a result of electron attachment, especially to oxygen molecules, leading to the demise of the avalanche. On the other hand, an avalanche could not grow continuously, without limit, even if the background electric field were to remain at a value higher than the critical value because, as the electron avalanche

propagates, low mobile positive space charge accumulates at the avalanche head. If the number of positive ions in the avalanche head becomes larger than a certain critical value, the electric field created by the space charge becomes comparable to the background electric field and the avalanche will transform into a streamer discharge. The critical electron number density that is necessary to convert an avalanche to a streamer is about $10^8 - 10^9$ (Gallimberti, 1979; Bazelyan and Raizer, 1998).

3. Electric radiation fields generated by a stream of electrons

The geometry relevant to the analysis presented in this manuscript is shown in Fig. 1. Assume that, at time $t=0$, a stream of electrons starts moving from point O along the z -axis with constant speed u . The current associated with the electron beam (i.e. the number of electrons emitted per second times the electronic charge) is given by $i_e(t)$. An expression for the radiation field generated by such an electron beam is derived by Cooray and Cooray (2010). According to their analysis, the radiation field at point P generated by the acceleration of electrons from rest to speed u at point O is given by

$$E(t) = \frac{i_e(t-r/c)u \sin \theta}{4\pi\epsilon_0 c^2 r} \frac{1}{[1 - \frac{u \cos \theta}{c}]} \mathbf{a}_\theta \tag{3}$$

By comparing this expression to other procedures that can be used to calculate radiation fields, its validity had been tested and confirmed by Cooray and Cooray (2010). In the analysis that follows, this equation will be used to calculate the radiation field of electron avalanches.

4. The electromagnetic fields of an electron avalanche

The geometry relevant to the derivation considered here is shown in Fig. 2. The electron avalanche starts with one electron at the origin and moves in the direction z . The background electric field, which is a function of z is denoted

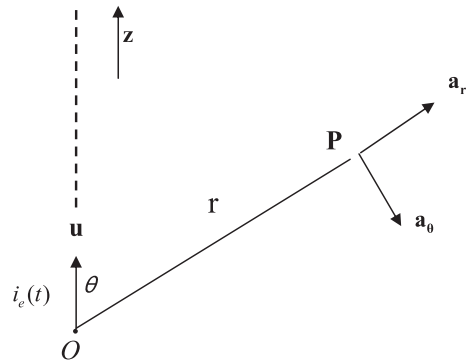


Fig. 1. Geometry pertinent to the parameters used in Eq. (3). The stream of electrons starts from O at time $t=0$ and all the electrons move with speed u in the z -direction. Note that $i_e(t)$ is the electron current and is negative according to standard convention.

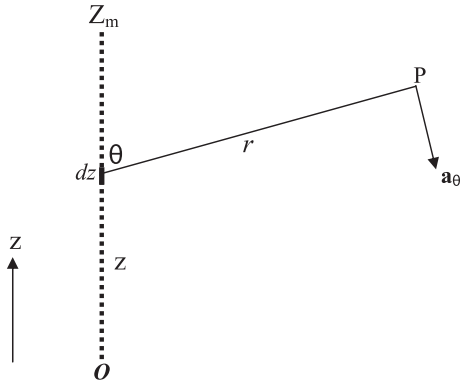


Fig. 2. Diagram pertinent to the calculation of radiation fields from an electron avalanche. The electron avalanche starts at O. The number density of electrons reaches the critical value at some point between O and Z_m and then continues to decay. The number of electrons in the avalanche goes to zero at $z = Z_m$.

by $E(z)$. Consider an element dz which is located at z . The number of electrons reaching the element dz is given by

$$n_e = \exp\left\{\int_0^z \bar{\alpha}(\xi) d\xi\right\}. \quad (4)$$

As these electrons travel along the element dz , they will give rise to additional electrons and the current corresponding to these new electrons is given by

$$dI_e(t) = e\delta[t - z/v_{av}(z)]\bar{\alpha}(z)dz \exp\left\{\int_0^z \bar{\alpha}(\xi) d\xi\right\} \quad (5)$$

where $v_{av}(z)$ is the average drift speed of electrons over the length 0 to z , e is the electronic charge and $\delta(t)$ is the Dirac Delta function. Noting that the additional electrons created in the element dz will be moving with drift velocity $v(z)$ at z , the radiation field at point P generated by this current can be written as

$$dE_e(t) = \frac{dI_e(t-r/c)v(z)\sin\theta}{4\pi\epsilon_0 c^2 r} \frac{1}{\left[1 - \frac{v(z)\cos\theta}{c}\right]} a_\theta. \quad (6)$$

Now, since the drift velocity is also a function of z , the speed of the electrons entering the element dz will change from $v(z)$ to $v(z+dz)$ in moving along the element dz . Now, the electric current entering the element dz is given by

$$dI_d(t) = e\delta(t - z/v_{av}(z)) \exp\left\{\int_0^z \bar{\alpha}(\xi) d\xi\right\}. \quad (7)$$

The radiation produced by the change in velocity is then given by

$$dE_d(t) = \frac{dI_d(t-r/c)[v(z+dz) - v(z)]\sin\theta}{4\pi\epsilon_0 c^2 r} \frac{1}{\left[1 - \frac{v(z)\cos\theta}{c}\right]} a_\theta. \quad (8)$$

Note that in writing down the above equation we have neglected the variation of $v(z)$ in the factor $1 - v(z)\cos\theta/c$ that appears in the denominator. Actually, this factor does not contribute much to the radiation field because the drift velocity of electrons in avalanches is orders of magnitude less than c . Now, Eq. (8) can be written as

$$dE_d(t) = \frac{\partial v(z)}{\partial z} dz \frac{dI_d(t-r/c)\sin\theta}{4\pi\epsilon_0 c^2 r} \frac{1}{\left[1 - \frac{v(z)\cos\theta}{c}\right]} a_\theta. \quad (9)$$

Thus the total radiation generated by the avalanche is given by

$$E(t) = \int_0^{z_{max}} dE_e(t) + \int_0^{z_{max}} dE_d(t) \quad (10)$$

where Z_{max} is the position at which the number of electrons in the avalanche goes to zero. Now let us consider the solution of these two integrals. One can perform the integrations analytically, provided that we assume that the point of observation is so far away that one can neglect the variation of r (both the magnitude and direction) over the avalanche length (the validity of this assumption is discussed further in Section 5). Making this assumption, changing the variable $t - z/v_{av}(z)$ to ζ and noting down that

$$dz = \frac{d\zeta}{\left[\frac{z_0}{v_{ave}^2(z_0)} \left\{\frac{\partial v_{ave}(z)}{\partial z}\right\}_{z=z_0} - \frac{1}{v_{ave}(z_0)}\right]} \quad (11)$$

one can write down the solutions of these equations directly, and the results are

$$E_e(t) = \frac{F(z_0)e\bar{\alpha}(z_0)v(z_0)\sin\theta}{4\pi\epsilon_0 c^2 r \left[1 - \frac{v(z_0)\cos\theta}{c}\right]} \exp\left\{\int_0^{z_0} \bar{\alpha}(\xi) d\xi\right\} a_\theta \quad (12)$$

$$F(z_0) = \frac{1}{\left[\frac{z_0}{v_{ave}^2(z_0)} \left\{\frac{\partial v_{ave}(z)}{\partial z}\right\}_{z=z_0} - \frac{1}{v_{ave}(z_0)}\right]} \quad (13)$$

with $z_0 = v_{av}(z)(t - r/c)$, where t is the time. Similarly, the solution of the second part of Eq. (10) is

$$E_d(t) = \frac{F(z_0)e\left\{\frac{\partial v(z)}{\partial z}\right\}_{z=z_0}\sin\theta}{4\pi\epsilon_0 c^2 r \left[1 - \frac{v(z_0)\cos\theta}{c}\right]} \exp\left\{\int_0^{z_0} \bar{\alpha}(\xi) d\xi\right\} a_\theta. \quad (14)$$

The total radiation field generated by the avalanche is given by

$$E(t) = \frac{F(z_0)e \left(\bar{\alpha}(z_0)v(z_0) + \left\{ \frac{\partial v(z)}{\partial z} \right\}_{z=z_0} \right) \sin\theta}{4\pi\epsilon_0 c^2 r \left[1 - \frac{v(z_0)}{c} \cos\theta \right]} \exp \left\{ \int_0^{z_0} \bar{\alpha}(\xi) d\xi \right\} a_\theta \quad (15)$$

Numerical calculation of these equations requires expressions for $\bar{\alpha}(z)$ and $v(z)$, however, as mentioned earlier, their values depend on the background electric field which varies along the z -axis. Denoting the gas density by N (in cm^{-3}) and the background electric field by E (in V/cm), these dependencies can be described by the following equations (Morrow, 1985; Morrow and Lowke, 1997).

$$\frac{\alpha}{N} = 2.0 \times 10^{-16} \exp \left[\left(-7.248 \times 10^{-15} \right) / (E/N) \right] \text{ cm}^2 \text{ for } E/N > 1.5 \times 10^{-15} \text{ V cm}^2 \quad (16)$$

$$\frac{\alpha}{N} = 6.619 \times 10^{-17} \exp \left[\left(-5.593 \times 10^{-15} \right) / (E/N) \right] \text{ cm}^2 \text{ for } E/N \leq 1.5 \times 10^{-15} \text{ V cm}^2 \quad (17)$$

$$\frac{\eta}{N} = 8.889 \times 10^{-5} (E/N) + 2.567 \times 10^{-19} \text{ cm}^2 \text{ for } E/N > 1.05 \times 10^{-15} \text{ V cm}^2 \quad (18)$$

$$\frac{\eta}{N} = 6.089 \times 10^{-4} (E/N) - 2.893 \times 10^{-19} \text{ cm}^2 \text{ for } E/N \leq 1.05 \times 10^{-15} \text{ V cm}^2 \quad (19)$$

$$v = 2.1569 \times 10^{16} (E/N)^{0.6064} \text{ cm/s.} \quad (20)$$

The set of equations given above completely defines the radiation field generated by the electron avalanche. As one can see from these equations, since $\bar{\alpha}$ and v depend on the background electric field, the growth of the electron avalanches must also depend on this field. Thus, depending on the magnitude and the spatial extent of the electric field, the avalanche may either cease growing after extending over a certain distance in space or it may grow to such an extent that it will form a streamer. An avalanche that barely satisfies the condition for converting itself into a streamer is called a critical avalanche. Once the avalanche becomes a streamer, the streamer starts propagating, creating critical avalanches at its tip. The collective action of such streamers can generate leader discharges which are the precursors to lightning discharges. Avalanches also play a main role in corona discharges. If, however, the magnitude and the spatial extent of the background field are not large enough, the corona discharge will be comprised of electron avalanches that do not reach the critical stage enabling them to become streamers. However, if the electric field associated with a corona discharge is increased beyond a certain value, the avalanches will convert to streamers, changing the form of the corona discharge.

In this paper we will confine ourselves to the calculation of the electric radiation fields of critical avalanches. Of course the equations can be used to calculate the radiation fields of any electron avalanche, irrespective of whether it reaches the critical condition or not. However, since the current associated with an avalanche that reaches the critical stage is larger than that for one that does not achieve that stage, the

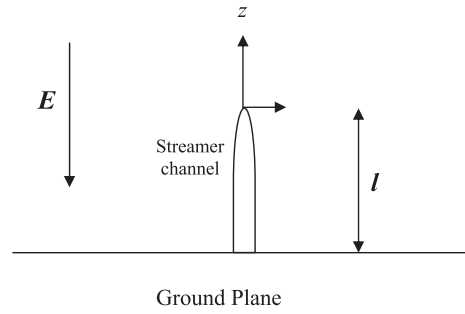


Fig. 3. Diagram pertinent to the calculation of radiation from a critical avalanche taking place at the head of a streamer. In the diagram l is the length of the streamer channel and E is the background electric field.

magnitude of the radiation field generated by critical avalanches would be larger than that produced by non-critical ones. So, in effect, the radiation field to be calculated in this paper is the maximum that can be produced by an electron avalanche. Moreover, since the spatial variation of the field depends on the geometric configuration, we will consider different geometries in the analysis.

5. Electron avalanches generated at the tip of a streamer discharge

In order to evaluate the growth of an avalanche at the tip of a streamer discharge, it is necessary to evaluate the electric field generated by the streamer. The basic configuration used in the analysis presented here is shown in Fig. 3. In the calculation the streamer channel is represented by a cylindrical region with a hemispherical tip. The radius of

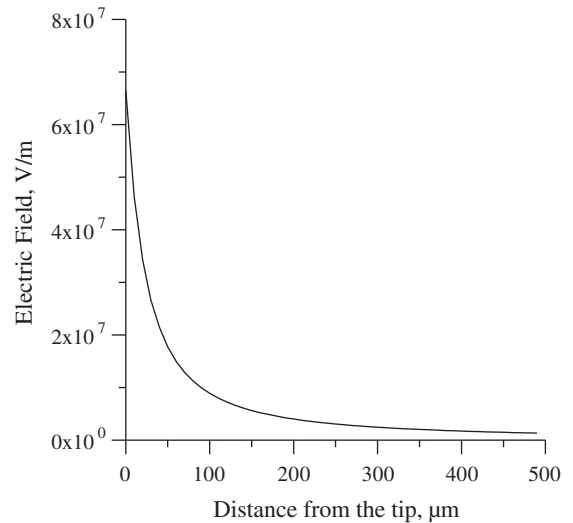


Fig. 4. The electric field in front of the head (or tip) of a 2 cm long streamer channel when the background electric field is equal to 575 kV/m . In the calculation, the potential gradient in the streamer channel is assumed to be 500 kV/m . In this electric field an electron starting at the head of the streamer channel will just reach the critical number density 10^{29} just before the electron density at the head of the avalanche starts to decay (i.e. critical electrical avalanche).

the streamer channel is taken to be $50\ \mu\text{m}$ and the potential gradient along the channel is assumed to be $500\ \text{kV/m}$ (Gallimberti, 1979). The streamer is assumed to emanate from a conducting plane (or electrode) above which exists a uniform background electric field. The charge simulation method (Steinbigler, 1969) is used to calculate the charge induced in the streamer channel and from this charge the field in front of the streamer is calculated. A detailed description of the method of calculation of the electric field in front of a streamer is described previously in Cooray et al. (2009). In the calculation, for a given streamer length, the background electric field is increased until the electric field at the tip of the streamer is barely enough to sustain a critical

avalanche. The number density of electrons in the critical avalanche, n_c , is assumed to be 10^9 (Bazelyan and Raizer, 1998). Fig. 4 shows the resulting electric field for a 2 cm long streamer channel. The corresponding background electric field is $575\ \text{kV/m}$. Note that the electric field decreases with distance, but its amplitude remains larger than $2.8 \times 10^6\ \text{V/m}$ over a length of about $200\ \mu\text{m}$. This is in agreement with the experimentally observed features of streamer discharges (Gallimberti, 1979). Thus, it is reasonable to assume that this electric field configuration reproduces the electric field experienced by avalanches growing in front of a streamer.

Using the field configuration determined above, we have evaluated how the charge on an avalanche grows as a function of the distance measured from the tip of the streamer. This information is then used in the equations given previously to calculate the radiation field. The resulting radiation field at a distance of 10 m from the avalanche is shown in Fig. 5a. Note that the duration of the radiation field is a few nanoseconds, and the rising part of the field has a rise time of about $0.25\ \text{ns}$. To the best of our knowledge, this is the first time that the radiation field generated by an electron avalanche has been evaluated and its time evolution documented. If the background electric field is below $575\ \text{kV/m}$, the avalanche will not grow to a critical size and, consequently, the radiation field will decrease. Of course, if the channels were longer, the background electric field necessary to drive an electron to a critical avalanche at a streamer tip would be smaller. Recall that in the calculation it was assumed that the electron number density of a critical avalanche, n_c , is equal to 10^9 . In order to illustrate the effect of this critical value another calculation was made for $n_c = 10^8$. The results are shown in Fig. 5b. Note that the amplitude of the radiation decreases with decreasing n_c .

It is important to mention here that, in performing the integration in Eq. (10) it was assumed that the point of observation is far away from the source so that the variation of r can be neglected over the limits of integration. In antenna theory, such an assumption is shown to be valid for amplitude terms that appear in the denominator of the field expressions but the terms that carry phase information cannot be simplified using this approximation if the antenna size is comparable to the relevant wavelengths. Let us consider the spatial extension of the avalanche with time. Calculations show that the extension of the avalanche over the first 2 ns, where the radiation field almost becomes zero, is about $0.2\ \text{mm}$. Thus, the assumption of neglecting the variation of r over the integral is valid for frequencies up to about 10–30 GHz.

6. Electron avalanches occurring in coaxial geometry

In a coaxial geometry, the electric field decreases as $1/r$, where r is the radial distance measured from the center of the coaxial arrangement. In performing the calculations, one could select a wide variety of geometries with different inner and outer radii. The calculation presented here is for a case which is of practical interest, however it should be noted that the procedure is equally valid for evaluating the avalanche radiation from any co-axial configuration. In the configuration selected, we assume the radius of the inner conductor to be $1\ \text{mm}$ and the outer radius to be $5\ \text{m}$. This configuration resembles to some extent the geometries of overhead power

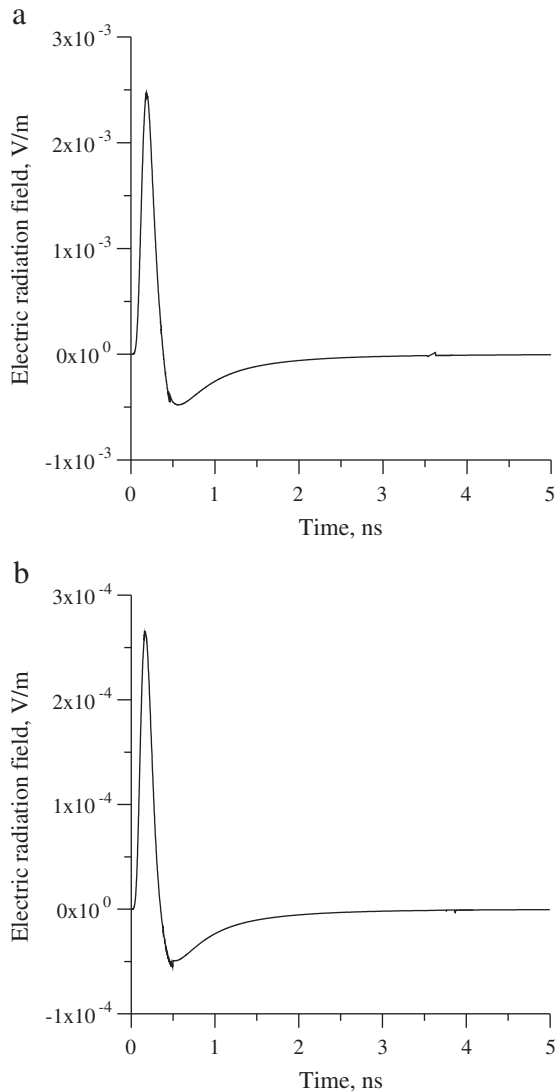


Fig. 5. The radiation field generated by a critical avalanche at a distance of 10 m from the avalanche. The depicted electric field is the direct field, i.e. without the contribution of the image in the conducting plane. The calculated fields correspond to $\theta = 90^\circ$. (a) For a critical avalanche of 10^9 electrons. (b) For a critical avalanche of 10^8 electrons.

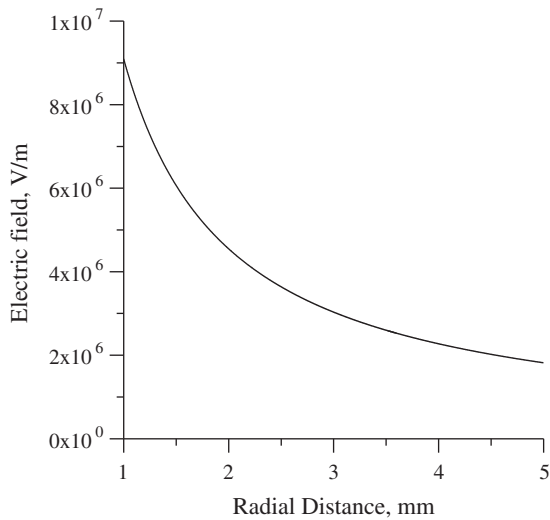


Fig. 6. The electric field in the coaxial configuration where electron avalanches take place. The radius of the inner conductor is 1 mm and that of the outer conductor is 5 mm. In this electric field an electron starting at the surface of the inner conductor will just reach the critical number density 10^9 before the electron density at the head of the avalanche starts to decay.

lines, which are of practical interest. In the analysis conducted here, the voltage of the inner conductor is raised until an electron released from the inner conductor will give rise to a critical avalanche. The resulting electric field is displayed as a function of radial distance from the conductor in Fig. 6. The radiation field generated by the growing avalanche in this field is calculated and the results are presented in Fig. 7a. Comparison of the data in Figs. 5 and 7a reveals that there are slight differences in the radiation fields of the avalanches in the two configurations, with the coaxial geometry resulting in a broader field with a larger overshoot. Of course, the shape of the radiation field also depends to some extent on the radius of the inner conductor. Just to illustrate the effect, another calculation was made with 0.01 cm being taken for the conductor radii. The results are shown in Fig. 7b. Note that with smaller radii the field decreases more rapidly with radial distance and, as a result, the creation of a critical avalanche requires a higher field at the surface of the conductor. This change in the amplitude of the field and its spatial variation change the growth rate of the avalanche causing the changes in the radiation field.

7. Electron avalanches in a spherical geometry

The spherical geometry is of interest when studying the generation of corona or streamers from water droplets or hail particles in thunderclouds. Although, the procedure for the calculation is the same, irrespective of the size of the particle, in the analysis presented here, the size of the sphere was taken to be 0.2 cm in diameter to simulate the size of water drops and hail particles in thunderclouds. In the calculation, the charge on the spherical particle is increased until the avalanche generated by an electron released from the surface will achieve the critical number density. The electric field

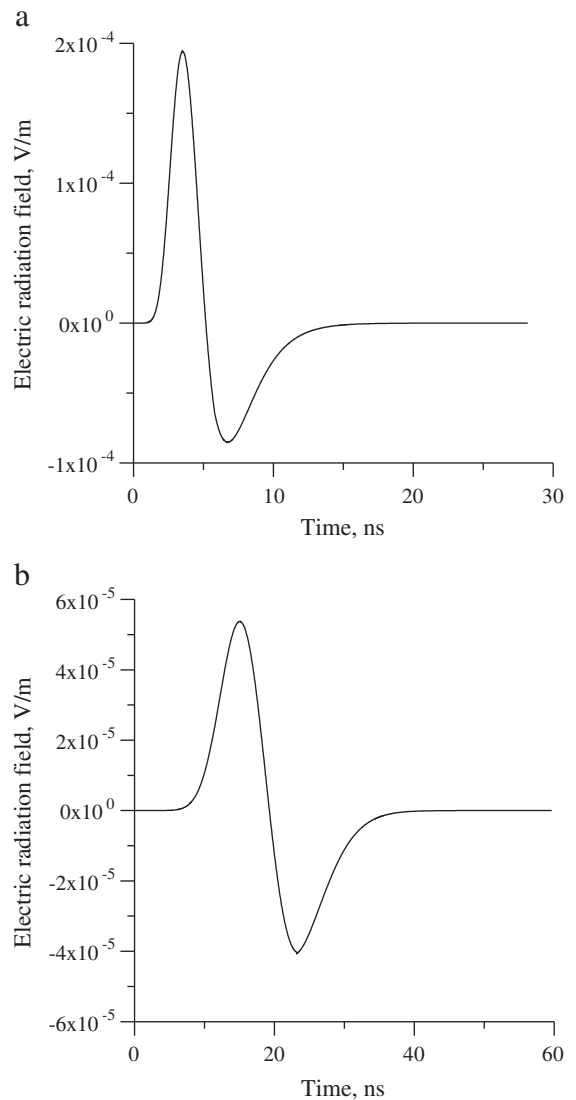


Fig. 7. Radiation field at 10 m produced by a critical avalanche growing in a coaxial configuration. (a) The inner radius of the coaxial configuration is equal to 1 mm. (b) The inner radius of the coaxial configuration is equal to 1 cm.

corresponding to this critical situation is displayed in Fig. 8. The resulting radiation field 10 m from the avalanche is reproduced in Fig. 9a. For comparison, another calculation was made taking a larger diameter and the resulting avalanche radiation is also plotted in Fig. 9b. Note that, as in the coaxial geometry, with an increased diameter the radiation field becomes broader and the overshoot becomes larger.

In the study it is assumed that only a one avalanche is generated from the sphere. In practice, it is possible that multiple avalanches could be generated and then the total field has to be calculated by summing up the contribution from all of them. However, the goal of the paper is to illustrate the radiation field of a single avalanche.

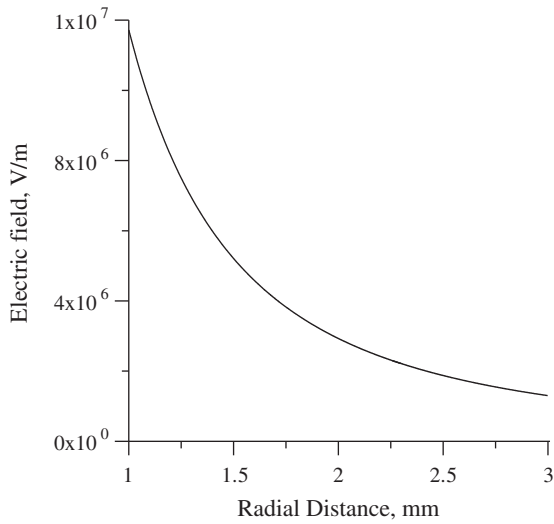


Fig. 8. The electric field as a function of the radial distance from a charged sphere where electron avalanches take place. The radius of the sphere is 1 mm. In this electric field an electron starting at the surface of the sphere will just reach the critical number density 10^9 before the electron density at the head of the avalanche starts to decay.

8. The frequency spectrum of avalanche radiation

The frequency spectrum, $F(\omega)$, of an electric field calculated or measured in the time domain is defined by the Fourier transformation as

$$F(\omega) = \int_0^{\infty} E(t)e^{-j\omega t} dt. \quad (21)$$

In the above equation, $E(t)$ is the calculated or measured electric field, ω is the angular frequency and $j^2 = -1$. One can use this equation in conjunction with the time domain electric fields given in Figs. 5, 7 and 9, to obtain the frequency spectrum of the avalanche radiation field. The amplitude spectrum of the avalanches is calculated here from the electric fields shown in Figs. 5a, 7a and 9a using Fourier transformation as defined by Eq. (21). The results, in dB, obtained for the three waveforms corresponding to pointed, co-axial and spherical geometry are presented in Fig. 10. Recall that the waveforms in the above figures were calculated at a distance of 10 m from the avalanche and, therefore, the frequency spectrum in Fig. 10 also corresponds to an electron avalanche at this distance. Note that the peak of the spectrum occurs around 1 GHz and then the spectral amplitude decreases rapidly with increasing frequency. Of course, since the duration of the radiation field is a few nanoseconds, one would expect the frequency spectrum of the avalanches to peak at frequencies close to a Gigahertz. In this respect, it is of interest to refer to the experiments conducted by Chauzy and Kably (1989). These authors have measured the current generated by electrical discharges between two spherical bodies, either metal spheres or water drops, separated by a distance of the order of millimeters. From the measured current, the time domain electric field and the corresponding spectrum were obtained.

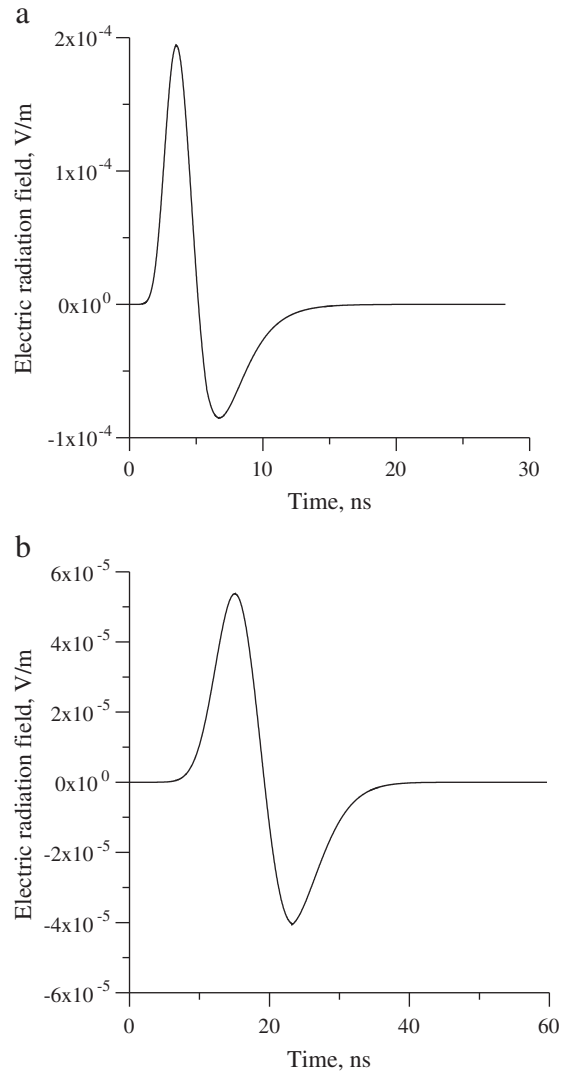


Fig. 9. Radiation field at 10 m produced by a critical avalanche growing in front of a charged sphere. (a) The radius of the sphere is equal to 1 mm. (b) The radius of the sphere is equal to 2 mm.

The cut-off frequency of the measuring system was 5×10^8 Hz and the calculated frequency spectrum peaked between 10^8 and 10^9 Hz. This is similar to the features of the frequency spectrum obtained for the avalanches. The reason for such a similarity could be the following. In the experiment, the length of the discharge is of the order of a millimeter. Since the distance over which the electrons can be accelerated is limited, it is possible that the discharge is predominantly mediated by electron avalanches, without the occurrence of streamers.

9. The frequency spectrum of atmospheric electrical discharges

Since all electrical discharges in the atmosphere created by natural processes are initiated and maintained by electron avalanches, it is reasonable to assume that the high frequency end of the electromagnetic spectrum of these discharges is

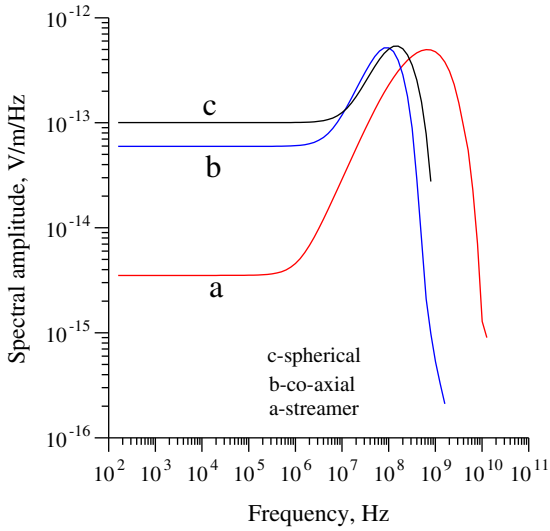


Fig. 10. Frequency spectrum of critical avalanches growing (a) in front of a streamer channel (corresponds to Fig. 5a), (b) in coaxial geometry (corresponds to Fig. 7a) and (c) spherical geometry (corresponds to Fig. 9a).

determined by the frequency spectrum of electron avalanches. Before proceeding further, let us derive an expression for the electromagnetic field of an avalanche located at a height h above a perfectly conducting ground. The geometry relevant to the calculation is shown in Fig. 11. Assume that the direction of the electron growth in the avalanche is along the z -axis. The radiation field produced by the avalanche at a horizontal distance D from the axis of the avalanche at ground level is given by

$$E(t) = \frac{F(z_0)e \left(\bar{\alpha}(z_0)v(z_0) + \left\{ \frac{\partial v(z)}{\partial z} \right\}_{z=z_0} \right) \sin^2 \theta}{2\pi\epsilon_0 c^2 r} \exp \left\{ \int_0^{z_0} \bar{\alpha}(\xi) d\xi \right\} \quad (22)$$

Note that, in the above equation, the presence of the perfectly conducting ground is taken care of by replacing the ground plane by the image of the avalanche.

Now, an atmospheric electrical discharge may contain a vast number of electron avalanches that are active throughout the whole discharge process. One can make a rough

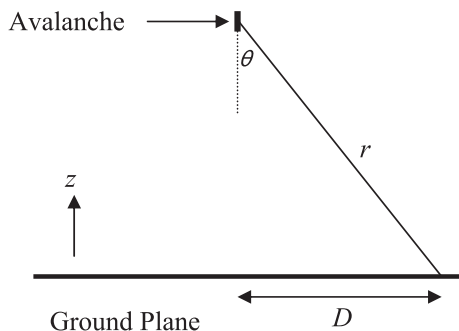


Fig. 11. Geometry relevant to the derivation of Eq. (22).

estimation of the contribution from all these avalanches to the electromagnetic spectrum of the discharge as follows: Consider a discharge process that transfers a charge of Q from one point in space to another. Since all electrical discharges are mediated by electron avalanches, it is reasonable to assume that this charge is transported at one stage or another by electrical avalanches. Let n_c be the critical number density of electrons in a critical avalanche. An electrical discharge transporting Q would, therefore, be involved in $Q/(en_c)$ avalanches. If the simplifying assumption is made that these avalanches occur randomly in time and that they do not overlap, the spectral contribution from avalanches is given by

$$F_q(\omega) = F_a(\omega) * \sqrt{Q / (en_c)}. \quad (23)$$

In the above equation $F_a(\omega)$ is the frequency spectrum of the electric radiation field produced by individual avalanches. However, a simple calculation shows that this assumption is not satisfied in the case of lightning flashes. Since the number of cloud flashes overwhelms the number of lightning flashes to ground in the Earth's atmosphere, let us consider a typical cloud flash. A typical cloud flash may neutralize about 30 C, and its typical duration is about 500 ms (Brook and Ogawa, 1977). Assuming that the transport of this charge is caused by critical avalanches at one stage or another, the total number of avalanches involved would be about 19×10^{10} (i.e. Q/en_c). Since the duration of an avalanche is about 1 ns, in order for the electric fields from individual avalanches not to interfere with each other, the total duration of the lightning flash has to be at least 190 s. However, this is obviously not the case, which shows that, in a lightning flash whose duration is about 500 ms, a significant number of avalanches will interfere with one another. In order to overcome this problem, let us make the physically reasonable assumption that the avalanches occur in bursts. In a given burst, the avalanches are located so close to each other in time that their electric fields are almost superimposed. However, different bursts are separated in time, so that the electric fields associated with one burst of activity do not interfere with the next. In this case the number of avalanches, N_a , that will occupy a single burst must be larger than or equal to

$$N_a \geq \frac{Qt_a}{en_c T_l}. \quad (24)$$

In the above equation, t_a is the duration of the avalanche and T_l is the duration of the lightning flash. The number of avalanche bursts in the flash, N_f is given by

$$N_f \leq \frac{T_l}{t_a}. \quad (25)$$

With these approximations, and considering the limiting values of N_a and N_f , the spectral contribution is given by

$$F_q(\omega) = F_a(\omega) * N_a \sqrt{N_f}. \quad (26)$$

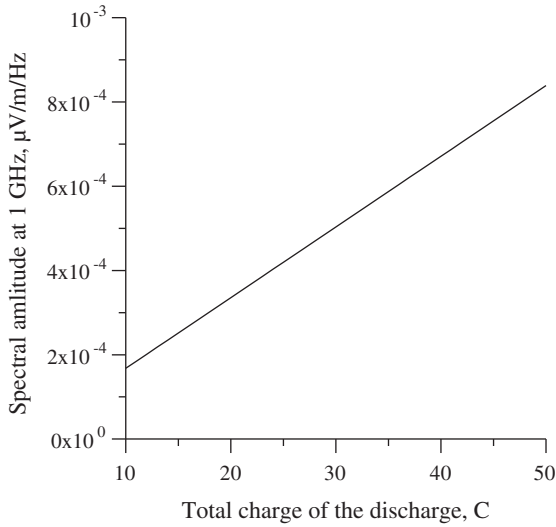


Fig. 12. The spectral amplitude at 1 GHz, normalized to 50 km, generated by the sum of avalanches taking place in a lightning discharge as a function of the neutralized charge. The assumptions made in the derivation are discussed in Section 9.

Substituting for N_a and N_f from Eqs. (24) and (25), respectively, one obtains

$$F_q(\omega) = F_a(\omega) \frac{Q}{en_c} \sqrt{\frac{t_a}{T_l}} \tag{27}$$

As mentioned previously, in the above equation $F_a(\omega)$ is the frequency spectrum of the individual avalanches. This can

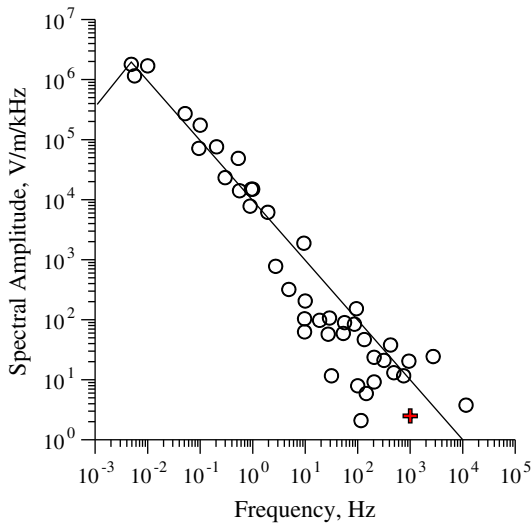


Fig. 13. The spectral characteristics of close lightning flashes normalized to a common distance of 10 km. The data points correspond to different measurements and the solid line shows the overall behavior. The cross represents the predicted contribution from avalanches. The diagram is adopted from Pierce (1977) and individual measurements are referenced in Oetzel and Pierce (1969).

be obtained by direct Fourier transformation of the time domain signal obtained from Eq. (22). In calculating the time domain signal using Eq. (22), the avalanches are assumed to take place at the head of the streamers. Thus the procedure for the calculation is identical to that given in Section 5. In Fig. 12, the calculated spectral component of the electromagnetic radiation field at 10^9 Hz for a measurement made at ground level at a distance of 50 km, is plotted as a function of charge Q assuming that the duration of the lightning flash remains at 500 ms irrespective of the charge. The height of the discharge from ground level is assumed to be 5 km. This distance corresponds roughly to the height at which the negative charge center is located in thunderclouds. Now, consider a typical cloud discharge. On average, it may transport a charge of about 30 C (Brook and Ogawa, 1977). Thus the spectral amplitude at 10^9 Hz can be calculated by substituting 30 C for Q in Eq. (27). The amplitude of the spectral component of 10^9 Hz thus calculated is plotted in Fig. 13 together with the narrow band amplitude spectrum of lightning flashes obtained from experimental observations as summarized by Pierce (1977). Observe that the experimental data are range normalized to a common distance of 10 km and the amplitudes are given in $\mu\text{V}/\text{m}/\text{kHz}$. It is important to stress that this calculation is an order of magnitude calculation because of several inherent assumptions. First, it was assumed that all avalanches in a given burst radiate in synchronization, which is not exactly correct. Second, it was assumed that all avalanches are directed in a vertical direction, but in reality they can have any orientation in space. Third, it was assumed that the duration of each burst is the same as the duration of an avalanche. In reality, the duration can be longer. Invalidity of the first two assumptions will lead to a decrease in the spectral amplitude, whereas the breakdown of the third assumption will lead to an increase in the spectral amplitude. Note also that, even though the parameter n_c appears in the denominator of Eq. (27), $F_q(\omega)$ is practically independent of n_c . The reason for this is that the calculated electric fields scale almost linearly with n_c and hence the quantity $F_a(\omega)/n_c$ is nearly independent of n_c .

Notwithstanding the assumptions mentioned above, it is interesting to note that the calculated value is in the same ballpark as the measured one at 10^9 Hz. This shows that radiation from electron avalanches may contribute a significant fraction to the lightning generated radiation around 10^9 Hz. Unfortunately, experimental data on the lightning electromagnetic spectrum around 10^9 Hz is scarce and more experimental data are needed around this frequency and beyond to determine the exact variation of the lightning electromagnetic spectrum in the vicinity of these frequencies.

10. Conclusions

In this paper the electromagnetic radiation fields created by electron avalanches were evaluated for electric fields in pointed, co-axial and spherical geometries. The results show that the radiation field has a duration of about 1–2 ns with a rise time of approximately 0.25 ns. The wave-shape has an initial peak followed by an overshoot in the opposite direction. The electromagnetic spectrum generated by the avalanches has a peak around 10^9 Hz.

References

- Bazelyan, E.M., Raizer, Y.P., 1998. Spark Discharge. CRC Press, New York.
- Brook, M., Ogawa, T., 1977. The cloud flash. In: Golde, R.H. (Ed.), *Lightning*, vol. 1. Academic Press, London, UK.
- Chauzy, S., Kably, K., 1989. Electric discharge between hydrometeors. *Journal of Geophysical Research* 94, 13,107–13,114.
- Cooray, V., 2003a. The mechanism of the lightning flash. In: Cooray, V. (Ed.), *The Lightning Flash*. The Institution of Electrical Engineers, London, UK.
- Cooray, V., 2003b. Mathematical modeling of return strokes. In: Cooray, V. (Ed.), *The Lightning Flash*. The Institution of Electrical Engineers, London, UK.
- Cooray, V., Cooray, G., 2010. The Electromagnetic Fields of an Accelerating Charge: Applications in Lightning Return-Stroke Models. *IEEE Transactions on Electromagnetic Compatibility* 52 (4), 944–955.
- Cooray, V., Arevalo, L., Rahman, M., Dwyer, J., Rassoul, H., 2009. On the possible origin of X-rays in long laboratory sparks. *Journal of Atmospheric and Solar-Terrestrial Physics* 71, 1890–1898.
- Gallimberti, I., 1979. The mechanism of long spark formation. *Journal of Physique of Colloque* 40 (C7), 193–250.
- Gardner, L., 1990. *Lightning Electromagnetics*. CRC Press, Florida, USA.
- Les Renardières Group, 1972. Research on long air gap discharges at Les Renardières. *Electra* 23, 53–157.
- Loeb, L.B., 1955. *Basic Processes of Gaseous Discharges*. University of California Press, Berkeley, California, USA.
- Morrow, R., 1985. Theory of negative corona in oxygen. *Physical Review A* 32, 1799–1809.
- Morrow, R., Lowke, J.J., 1997. Streamer propagation in air. *Journal of Physics D: Applied Physics* 30, 614–627.
- Oetzel, G.N., Pierce, E.T., 1969. The radio emissions from close lightning. In: Coroniti, S.C., Hughes, J. (Eds.), *Planetary Electrodynamics*, vol. 1. Gordon and Breach, New York.
- Pierce, E.T., 1977. Atmospheric and radio noise. In: Golde, R.H. (Ed.), *Lightning*, vol. 1. Academic Press, London, UK.
- Raizer, Y.P., 1991. *Gas Discharge Physics*. Springer, Berlin, Germany.
- Rakov, V.A., Uman, M.A., 2003. *Lightning—Physics and Effects*. Cambridge University Press, Cambridge, UK.
- Steinbigler, H., 1969. Anfangsfeldstärken und Ausnutzungsfaktoren rotations-symmetrischer Elektrodenanordnungen in luft, Dissertation, TH Munich, Germany.
- Thottappillil, R., Rakov, V.A., 2001. On different approaches to calculating lightning electric fields. *Journal of Geophysical Research* 106, 14191–14205.
- Townsend, J.S., 1915. *Electricity in Gases*. Oxford University Press, Oxford, UK.